

Highlighting research results from the lab of
Molecular Photochemistry & Photophysics,
State Key Laboratory of Fine Chemicals, Dalian
University of Technology, China.

Title: Tuning the photophysical properties of N^N Pt(II)
bisacetylides with fluorene moiety and its applications
for triplet-triplet-annihilation based upconversion

A series of N^N Pt(II) bisacetylides complexes, with
fluorene-containing aryl acetylides ligands, were prepared
and used for triplet-triplet annihilation (TTA) upconversion.
We proposed that non-phosphorescent transition metal
complexes can also be used as the triplet sensitizers.

As featured in:



See Q. Li *et al.*,
J. Mater. Chem., 2012, **22**, 5319.

RSC Publishing

www.rsc.org/materials

Registered Charity Number 207890

Tuning the photophysical properties of $N^{\wedge}N$ Pt(II) bisacetylide complexes with fluorene moiety and its applications for triplet–triplet-annihilation based upconversion†

Qiuting Li, Huimin Guo,* Lihua Ma, Wanhua Wu, Yifan Liu and Jianzhang Zhao*

Received 5th November 2011, Accepted 24th November 2011

DOI: 10.1039/c2jm15678d

Fluorene-containing aryl acetylide ligands were used to prepare $N^{\wedge}N$ Pt(II) bisacetylide complexes, where aryl substituents on the fluorene are phenyl (**Pt-1**), naphthal (**Pt-2**), anthranlyl (**Pt-3**), pyrenyl (**Pt-4**), 4-diphenylaminophenyl (**Pt-5**) and 9,9-di-*n*-octylfluorene (**Pt-6**) (where $N^{\wedge}N$ ligand = 4,4'-di-*tert*-butyl-2,2'-bipyridine, dbbpy). All the complexes show room temperature (RT) phosphorescence. The emissive T_1 excited states of **Pt-1**, **Pt-5** and **Pt-6** were assigned as metal-to-ligand-charge-transfer state (3 MLCT), whereas for **Pt-2**, **Pt-3** and **Pt-4**, the emissive T_1 excited states were identified as the intraligand state (3 IL), based on steady state emission spectra, the lifetime of the T_1 state, emission spectra at 77 K, spin density analysis and the time-resolved transient absorption spectroscopy. Exceptionally long lived T_1 excited state was observed for **Pt-3** ($\tau = 66.7 \mu\text{s}$) and **Pt-4** ($\tau = 54.7 \mu\text{s}$), compared to a model complex dbbpy Pt(II) Bisphenylacetylide ($\tau = 1.25 \mu\text{s}$). RT phosphorescence of anthracene was observed at 780 nm with **Pt-3**. The critical role of the fluorene is to move the absorption of the complexes to the red-end of the spectra, but at the same time, without compromising the energy level of the T_1 state of the complexes. The advantage of this unique spectral tuning effect and the long-lived T_1 excited states of **Pt-4** was demonstrated by the enhanced performance of the complexes as triplet sensitizers for triplet–triplet annihilation (TTA) based upconversion; an upconversion quantum yield (Φ_{UC}) up to 22.4% was observed with **Pt-4** as the sensitizer. Other complexes described herein show negligible upconversion. The high upconversion quantum yield of **Pt-4** is attributed to its intense absorption of visible light and long-lived T_1 excited state. Based on the result of **Pt-4**, we propose that weakly phosphorescent, or non-phosphorescent transition metal complexes can be used as triplet sensitizers for TTA upconversion, compared to the phosphorescent triplet sensitizers currently used for TTA upconversion. Our results will be useful for the design of transition metal complexes to enhance the light-absorption and thereafter the cascade photophysical processes, without decreasing the T_1 excited state energy levels, which are important for the application of the complexes as triplet sensitizers in various photophysical processes.

Introduction

Recently Pt(II) acetylide complexes have attracted much attention,¹ due to their applications in photocatalysis,² photoinduced charge separation,³ optical limiting,⁴ molecular probes,^{5–8} etc. Representative complexes are $N^{\wedge}N$ Pt(II) bisacetylide complexes, for which room temperature (RT) phosphorescence

was usually observed upon photoexcitation.^{1,9,10} The photophysical properties of the $N^{\wedge}N$ Pt(II) bisacetylide complexes, such as the UV-vis absorption, the emission wavelength and the lifetime of the T_1 excited state, are dependent on the structure of the acetylide ligand which is attached to the Pt(II) center.^{1,9–11} Thus the photophysical properties of Pt(II) acetylide complexes can be tuned by changing the acetylides. To date phenyl-acetylide or substituted phenylacetylides, naphthal and pyrenyl were attached to the Pt(II) center. Recently, we attached naphthalimide (NI),^{12,13} coumarin,¹⁴ and naphthalidimide (NDI) acetylide to the Pt(II) center of $N^{\wedge}N$ Pt(II) bisacetylide complexes,¹⁵ and we observed exceptionally long triplet excited state lifetimes and room temperature near-IR emission of the emissive 3 IL excited state of the complexes.^{12,15}

However, much room is left for fine tuning the photophysical properties of the Pt(II) complexes. For example, (1) the UV-vis

State Key Laboratory of Fine Chemicals, School of Chemical Engineering, Dalian University of Technology, E-208 Western Campus, 2 Ling-Gong Road, Dalian, 116024, P. R. China. E-mail: guohm@dut.edu.cn; zhaojzh@dut.edu.cn; Web: <http://lfinechem.dlut.edu.cn/photochem>; Fax: +86 0411 84986236; Tel: +86 0411 84986236

† Electronic supplementary information (ESI) available: ^1H and ^{13}C NMR, and MS spectra. Absorption and emission spectra, upconversion and DFT calculation details. See DOI: 10.1039/c2jm15678d

absorption of the Pt(II) acetylide is usually weak in the visible region;^{1,9,10} (2) the T₁ excited state lifetime is short (less than 5 μs);^{1,9,10} (3) the difficulty to move the absorption to the red-end of the spectrum with ligand modification, but without any significant decrease of the T₁ excited state energy level. Recently we proved that with ligand modification, the UV-vis absorption band of the Pt(II) acetylide complexes can be drastically red-shifted, but the T₁ energy level decreased sharply.¹⁵ This decrease is detrimental to the application of the transition metal complexes because the matched triplet energy acceptor will be limited. Thus, it is desired to develop a strategy to move the UV-vis absorption of the complexes to the red-end, but at the same time, without compromising the high T₁ state energy levels. We propose that ligand modification with a specific chromophore is one of the promising approaches to address this challenge.

On the other hand, fluorene is a robust chromophore, due to its emission and charge carrier property, and has been extensively used in luminescent materials,^{16–19} electroluminescent materials,²⁰ optical limiting,^{21,22} and molecular probes.²³ To the best of our knowledge, however, the acetylide fluorene moiety has never been attached to the Pt(II) center of *N*[^]*N* Pt(II) bisacetylide complexes.¹ Herein for the first time we attached the fluorene chromophore to the Pt(II) center of the *N*[^]*N* Pt(II) bisacetylide complexes and importantly, we found that the aforementioned challenge, that is, to move the absorption to the red-end of the spectra and maintain the T₁ excited state energy level, can be addressed to some extent. Prolonged triplet excited state lifetimes were observed, especially for the complexes containing pyrenyl and anthranyl fluorene ligands (τ_T is up to 66.7 μs, compared to 1.36 μs of a parent complex). The photophysical properties of the complexes were studied with steady state, time-resolved spectroscopy and density-functional theory (DFT) calculations. ³IL emissive triplet excited states were proposed to be responsible for the anthracene and pyrenyl-containing complexes. The complexes were used as triplet sensitizers for triplet–triplet annihilation (TTA) based upconversion and an upconversion quantum yield (Φ_{UC}) up to 22.4% was observed. We propose that weakly phosphorescent or non-phosphorescent transition metal complexes can be used as triplet sensitizers for the TTA upconversion.

Experimental

General information

NMR spectra were taken on a 400 MHz Varian Unity Inova spectrophotometer. Mass spectra were recorded with a Q-TOF Micro MS spectrometer. UV-Vis spectra were taken on a HP8453 UV-visible spectrophotometer. Fluorescence spectra were recorded on a Shimadzu RF5301 fluorospectrometer and a Sanco 970 CRT spectrofluorometer. Luminescence quantum yields were measured with quinine sulfate as the standard (Φ = 54.6% in 0.05 M H₂SO₄). Luminescence lifetimes were measured on a Horiba Jobin Yvon Fluoro Max-4 and OB 920 luminescence lifetime spectrometer (Edinburgh, UK).

Diode pumped solid state laser (CW) was used for the upconversions. The samples were purged with N₂ or Ar for 15 min before measurement. The upconversion quantum yields were determined with coumarin-6 as the quantum yield standard (Φ =

78.0% in CH₃CH₂OH) and the quantum yields were calculated with eqn (1), where Φ_{unk}, A_{unk}, I_{unk} and η_{unk} represent the quantum yield, absorbance, integrated photoluminescence intensity and the refractive index of the samples. The photographs of the upconversion were taken with a Samsang NV 5 digital camera.

$$\Phi_{\text{unk}} = 2\Phi_{\text{std}} \left(\frac{A_{\text{std}}}{A_{\text{unk}}} \right) \left(\frac{I_{\text{unk}}}{I_{\text{std}}} \right) \left(\frac{\eta_{\text{unk}}}{\eta_{\text{std}}} \right)^2 \quad (1)$$

The DFT calculations were used for optimization of the singlet states and triplet states. The spin density surfaces of the complexes were calculated based on the optimized triplet state geometries. All the calculations were performed with Gaussian 09W.²⁴

2,7-Dibromofluorene (1)

A 100 mL two-necked flask equipped with a magnetic stirrer bar and a dropping funnel was loaded with fluorene (10.0 g, 60.2 mmol) and CHCl₃ (32 mL). The solution was stirred and bromine (7.2 mL, 140.4 mmol) in CHCl₃ (8.0 mL) was added dropwise. The solution was stirred at room temperature for 20 h in the dark. The solid material was filtered and washed with CHCl₃ (70 mL). The product was re-crystallized from CHCl₃. A white solid was obtained, 17.8 g, yield 92.2%. ¹H NMR (400 MHz, CDCl₃): δ 7.62 (s, 2H), δ 7.55 (d, 2H, *J* = 8.0 Hz), δ 7.48 (d, 2H, *J* = 8.0 Hz), δ 3.80 (s, 2H). ESI-MS C₁₃H₈Br₂ calculated *m/z* = 321.8993, found *m/z* = 321.9002.

9,9-Dioctyl-2,7-dibromofluorene (2)

2,7-Dibromofluorene (9.0 g, 27.8 mmol), tetrabutyl ammonium bromide (0.9 g, 2.70 mmol), 50% aqueous NaOH (45 mL), and toluene (60 mL) were mixed. The mixture was stirred under N₂ and then octylbromide (13.4 g, 69.3 mmol) was added. The mixture was stirred and heated at 60 °C for 4 h. The reaction mixture was extracted with ethyl acetate, then washed with water, and dried over Na₂SO₄. The solvent was evaporated and a clear yellow viscous product was obtained. The crude product was crystallized from absolute ethanol to give 2,7-dibromo-9,9-dioctylfluorene, 11.4 g, yield 75.0%. ¹H NMR (400 MHz, CDCl₃): δ 7.52 (d, 2H, *J* = 12.0 Hz), δ 7.46 (d, 2H, *J* = 4.0 Hz), δ 7.44 (s, 2H), δ 1.93–1.88 (m, 4H), δ 1.26–0.81 (m, 20H), δ 0.6–0.56 (m, 4H). ESI-MS C₂₉H₄₀Br₂ calculated *m/z* = 546.1503, found *m/z* = 546.1497.

1-(2-(2-Ethynyl-9,9-dioctyl-9H-fluoren-7-yl)ethynyl)-benzene (3a)

Phenylacetylene (0.10 g, 1.00 mmol), **2** (2.73 g, 5.00 mmol), CuI (10.0 mg, 0.05 mmol), Pd(PPh₃)₂Cl₂ (3.5 mg, 0.005 mmol), triphenylphosphine (5.0 mg, 0.02 mmol), and dry triethylamine (150 mL) were placed in a 250 mL round bottom flask. After the solution was purged with N₂ for 30 min, the mixture was stirred and refluxed under N₂ for 4 h. Then the reaction mixture was filtered and the filtrate was evaporated under reduced pressure. The residue was purified by column chromatography (silica gel, hexane). A white solid was obtained, 360.0 mg, yield: 63.4%. ¹H NMR (400 MHz, CDCl₃): δ 7.65 (d, 1H, *J* = 8.0 Hz), δ 7.57–7.47

(m, 3H), δ 7.38 (d, 4H, $J = 8.0$ Hz), δ 1.96–1.93 (m, 4H), δ 1.22–1.01 (m, 20H), δ 0.87–0.81 (m, 6H), δ 0.59–0.56 (m, 4H). ESI-MS $C_{37}H_{45}Br$ calculated $m/z = 568.2705$, found $m/z = 568.2705$.

1-(7-Ethynyl-9,9-dioctyl-9H-fluoren-2-yl)ethynylbenzene (L-1)

3a (284.0 mg, 0.50 mmol), 3-methyl-1-butyn-3-ol (63.0 mg, 0.75 mmol), CuI (5.0 mg, 0.025 mmol), Pd(PPh₃)₂Cl₂ (1.8 mg, 0.0025 mmol), triphenylphosphine (2.5 mg, 0.01 mmol), and dry triethylamine (50 mL) were placed in a 100 mL round bottom flask. After the solution was purged with N₂ for 30 min, it was stirred and refluxed for 8 h. The reaction mixture was filtered, and the filtrate was evaporated under reduced pressure. The residue was purified by column chromatography (silica gel, hexane : dichloromethane = 1 : 10, v/v) to give **P-1**. Then **P-1**, KOH (250.0 mg), and 2-propanol (50 mL) were added in a 100 mL round bottom flask. After the solution was purged with N₂ for 30 min, it was stirred and refluxed for 4 h. The solution was then washed with water and the aqueous phase was extracted with CH₂Cl₂ (3 × 30 mL). The solvent was evaporated under reduced pressure and the crude product was purified by column chromatography (silica gel, hexane) to give yellow oily **L-1**, 238.0 mg, yield 78.0%. ¹H NMR (400 MHz, CDCl₃): δ 7.67 (t, 3H, $J = 8.0$ Hz), δ 7.58 (d, 1H), δ 7.56 (d, 1H), δ 7.54 (s, 1H), δ 7.51 (d, 1H, $J = 4.0$ Hz), δ 7.48 (d, 1H, $J = 4.0$ Hz), δ 7.38–7.35 (m, 3H), δ 3.16 (s, 1H), δ 1.98–1.94 (m, 4H), δ 1.26–1.04 (m, 20H), δ 0.86–0.80 (m, 6H), δ 0.59–0.56 (m, 4H). ¹³C NMR (100 MHz, CDCl₃): δ 151.3, 141.4, 140.7, 131.8, 131.4, 130.9, 128.6, 126.7, 126.2, 123.4, 122.3, 120.8, 120.1, 94.6, 90.5, 89.9, 84.8, 55.4, 40.5, 32.0, 30.1, 29.4, 23.9, 22.8, 14.3. HR-MALDI-MS: $C_{39}H_{46}$ calculated $m/z = 514.3600$, found $m/z = 514.3605$.

Pt-1

Pt(dbbpy)Cl₂ (50.0 mg, 0.09 mmol), CuI (5.0 mg, 0.019 mmol) and diisopropylamine (1.0 mL) were dissolved in 5 mL CH₂Cl₂, the mixture was stirred for 10 min. The mixture was purged with Ar, **L-1** (138.0 mg, 0.27 mmol) was added and the mixture was stirred at r.t. for 24 h. The mixture was evaporated to dryness, the residue was purified by column chromatography (silica gel, CH₂Cl₂ : hexane = 1 : 1, v/v). The product was collected as the third fraction. 102.0 mg of yellow powder was obtained, yield: 76.0%. ¹H NMR (400 MHz, CDCl₃): δ 9.82 (d, 2H, $J = 4.0$ Hz), δ 7.99 (s, 2H), δ 7.63 (d, 6H, $J = 8.0$ Hz), δ 7.58–7.54 (m, 8H), δ 7.51–7.48 (m, 4H), δ 7.36 (m, 6H), 1.98–1.95 (m, 8H), δ 1.47 (s, 18H), δ 1.21–1.05 (m, 40H), δ 0.82–0.79 (m, 12H), δ 0.62–0.58 (m, 8H). ¹³C NMR (100 MHz, CDCl₃): δ 163.5, 156.4, 151.2, 150.7, 141.9, 138.0, 131.7, 130.7, 128.5, 128.2, 127.0, 126.0, 120.8, 119.5, 119.4, 119.0, 103.4, 91.1, 89.3, 87.3, 55.2, 40.8, 36.0, 32.0, 30.4, 29.5, 24.0, 22.8, 14.3. HR-MALDI-MS: $C_{96}H_{114}N_2Pt$ calculated $m/z = 1489.8630$, found, $m/z = 1489.8531$.

Pt-2

Pt-2 was prepared with a method similar to that used for **Pt-1** and obtained as a yellow solid, 105.0 mg, yield: 73.4%. ¹H NMR (400 MHz, CDCl₃): δ 9.84 (d, 2H, $J = 8.0$ Hz), δ 8.54 (d, 2H, $J = 8.0$ Hz), δ 7.89 (s, 2H), δ 7.90–7.80 (m, 6H), δ 7.67–7.58 (m, 18H), δ 7.50–7.46 (m, 2H), δ 2.03–1.99 (m, 8H), δ 1.47 (s, 18H), δ 1.22–1.08 (m, 40H), δ 0.82–0.79 (m, 12H), δ 0.69–0.63 (m, 8H). ¹³C

NMR (100 MHz, CDCl₃): δ 163.5, 156.4, 151.3, 150.7, 142.1, 138.0, 133.4, 131.4, 130.9, 130.4, 128.7, 127.8, 126.6, 125.5, 124.9, 121.4, 121.0, 119.6, 119.4, 119.9, 103.5, 96.0, 87.5, 55.3, 40.8, 36.0, 32.0, 30.4, 29.5, 24.0, 22.8, 14.3. HR-MALDI-MS: $C_{104}H_{118}N_2Pt$ calculated $m/z = 1590.8943$, found $m/z = 1589.8973$.

Pt-3

Pt-3 was prepared with similar method of **Pt-1**. Yellow solid, 90.0 mg, yield: 59.2%. ¹H NMR (400 MHz, CDCl₃): δ 9.85 (d, 2H, $J = 8.0$ Hz), δ 8.75 (d, 4H, $J = 8.0$ Hz), δ 8.44 (s, 2H), δ 8.05 (d, 4H, $J = 8.0$ Hz), δ 7.99 (s, 2H), δ 7.75–7.73 (m, 4H), δ 7.68–7.59 (m, 14H), δ 7.56 (t, 4H, $J = 8.0$ Hz), δ 2.07–2.04 (m, 8H), δ 1.48 (s, 18H), δ 1.20–1.11 (m, 40H), δ 0.74–0.67 (m, 12H), δ 0.62–0.60 (m, 8H). ¹³C NMR (100 MHz, CDCl₃): δ 163.6, 156.4, 151.5, 150.8, 142.2, 138.0, 132.7, 131.5, 130.9, 128.9, 127.8, 127.1, 126.7, 125.9, 124.9, 121.3, 119.7, 119.5, 118.9, 117.9, 102.6, 87.2, 86.3, 55.4, 40.9, 36.0, 30.5, 29.6, 24.0, 22.8, 14.3. HR-MALDI-MS: $C_{112}H_{122}N_2Pt$ calculated, $m/z = 1689.9256$, found $m/z = 1689.9415$.

Pt-4

Pt-4 was prepared with a method similar to that used for **Pt-1** and obtained as a yellow solid, 115.0 mg, yield: 78.2%. ¹H NMR (400 MHz, CDCl₃): δ 9.85 (d, 2H, $J = 4.0$ Hz), δ 8.77 (d, 2H, $J = 8.0$ Hz), δ 8.27–8.21 (m, 8H), δ 8.17 (d, 2H, $J = 8.0$ Hz), δ 8.10–8.04 (m, 6H), δ 7.99 (s, 2H), δ 7.70 (s, 4H), δ 7.65–7.60 (m, 8H), δ 1.46 (s, 18H), δ 1.19–1.09 (m, 40H), δ 0.82–0.79 (m, 12H), δ 0.71–0.65 (m, 8H). ¹³C NMR (100 MHz, CDCl₃): δ 163.4, 156.3, 151.2, 150.6, 142.0, 137.9, 131.8, 131.2, 131.1, 130.8, 129.6, 128.3, 128.0, 127.7, 127.3, 126.9, 125.8, 125.6, 124.7, 124.6, 124.4, 121.0, 119.3, 118.7, 118.3, 55.2, 40.7, 35.8, 31.9, 31.6, 30.3, 29.7, 29.4, 29.4, 23.9, 22.7, 14.1. HR-MALDI-MS: $C_{116}H_{122}N_2Pt$ calculated $m/z = 1737.9256$, found $m/z = 1737.9130$.

Pt-5

Pt-5 was prepared with a method similar to that used for **Pt-1** and obtained as a yellow solid, 30.0 mg, yield: 60.9%. ¹H NMR (400 MHz, CDCl₃): δ 9.82 (d, 2H, $J = 4.0$ Hz), δ 7.97 (s, 2H), δ 7.62–7.53 (m, 10H), δ 7.47 (d, 4H, $J = 8.0$ Hz), δ 7.42 (d, 4H, $J = 8.0$ Hz), δ 7.30 (m, 6H), δ 7.13 (d, 8H, $J = 8.0$ Hz), δ 7.08–7.01 (m, 8H), δ 1.19–1.94 (m, 8H), δ 1.46 (s, 18H), δ 1.21–1.05 (m, 40H), δ 0.82–0.79 (m, 12H), δ 0.65–0.59 (m, 8H). ¹³C NMR (100 MHz, CDCl₃): δ 163.4, 156.3, 151.3, 151.0, 150.5, 147.7, 147.3, 141.5, 137.9, 132.5, 131.1, 130.4, 129.4, 127.4, 126.9, 125.7, 124.9, 123.5, 122.5, 121.0, 119.2, 118.7, 116.5, 90.1, 89.4, 86.6, 55.0, 40.6, 35.8, 31.8, 30.3, 29.7, 29.4, 23.8, 22.6, 14.1. HR-MALDI-MS: $C_{120}H_{132}N_4Pt$ calculated $m/z = 1824.0100$, found $m/z = 1824.0171$.

Complex Pt-6

Pt-6 was prepared with a method similar to that used for **Pt-1**. Yellow solid 40.5 mg, yield: 52.6%. ¹H NMR (400 MHz, CDCl₃): δ 9.82 (d, 2H, $J = 8.0$ Hz), δ 7.98 (s, 1H), δ 7.70–7.68 (m, 5H), δ 7.65–7.59 (m, 8H), δ 7.57–7.52 (m, 9H), δ 7.33–7.32 (m, 6H), δ 2.00–1.96 (m, 16H), δ 1.46 (s, 18H), δ 1.20–1.05 (m, 80H),

δ 0.83–0.80 (m, 24H), δ 0.66–0.60 (m, 16H). ^{13}C NMR (100 MHz, CDCl_3): δ 163.4, 156.3, 151.3, 151.1, 150.8, 150.5, 141.7, 141.2, 140.5, 137.9, 131.2, 130.6, 127.4, 126.9, 125.9, 124.7, 122.9, 121.7, 120.9, 120.0, 119.6, 119.4, 119.2, 103.4, 90.8, 90.1, 86.8, 55.1, 40.7, 40.4, 35.8, 31.9, 30.8, 30.3, 30.1, 29.7, 29.4, 29.3, 23.8, 23.7, 22.6, 14.1. HR-MALDI-MS: $\text{C}_{142}\text{H}_{182}\text{N}_2\text{Pt}$ calculated $m/z = 2114.4264$, found $m/z = 2114.4287$.

Results and discussion

Design and synthesis of complexes

The design rationales of the fluorene-containing complexes (Scheme 1) are (1) different aryl acetylide ligands were attached to the fluorene moiety to tune the UV-vis absorption and to investigate the T_1 state energy levels; (2) alkyl chains were introduced to the fluorene moieties to improve the solubility of the complexes; (3) pyrene and anthracene moieties were introduced with the intention to observe the long-lived ^3IL triplet excited state.^{15,25–28} Fluorene was used as the starting material (Scheme 1). After bromination and introduction of the alkyl chain, acetylide moieties were attached by using the Sonogashira cross-coupling reactions. All the complexes were obtained in excellent to moderate yields.

Absorption and emission spectra

The UV-vis absorption of the ligands was studied (Fig. 1a). Ligands **L-1**, **L-2** and **L-6** give absorption in the UV region. Ligands with anthracene, pyrene and triphenylamine moieties show absorption extended to 440 nm.

The UV-vis absorption of the complexes was also studied (Fig. 1b). Intense absorption in the visible region was observed for **Pt-3** and **Pt-4**. The molar extinction coefficient is up to $8.54 \times 10^4 \text{ M}^{-1} \text{ cm}^{-1}$ for **Pt-3** at 445 nm. For **Pt-4**, ϵ is $9.70 \times 10^4 \text{ M}^{-1} \text{ cm}^{-1}$ at 420 nm. It should be pointed out that the normal Pt(II) bisacetylide complexes show weak absorption in the visible region.^{9–11,29} Interestingly, we found that the fluorene-containing complexes show red-shifted absorption compared to that of the analogues without the fluorene moiety. For example, **Pt-4** shows absorption at 420 nm. By comparison, the dbbpy Pt(II) bispyrenylacetylide complex shows weak and blue-shifted absorption.²⁵ **Pt-1** also shows enhanced and red-shifted absorption than the model complex dbbpy Pt(II) bisphenylacetylide.¹⁰ The enhanced absorption of the complexes in the visible region will be beneficial for the applications.

The emissions of the ligands and the complexes were studied (Fig. 2). The ligands show intense fluorescence emission in the range of 350–500 nm (Fig. 2a). Intense room temperature (RT) emissions were observed for **Pt-1**, **Pt-2**, **Pt-5** and **Pt-6**. The emission maximum of these complexes is similar, located at 585 nm. Furthermore, these complexes show similar phosphorescent quantum yields (Table 1). Thus we propose that these complexes share the similar emissive triplet excited states (T_1 excited state). For complexes **Pt-3** and **Pt-4**, however, much weaker emission was observed ($\Phi = 0.0\%$ and 0.3% , respectively). Furthermore, the emission band of **Pt-4** is more structured than the emission bands of **Pt-1**, **Pt-2**, **Pt-5** and **Pt-6**, which is a clear indication of an emissive state with significant ^3IL feature, not the normal $^3\text{MLCT}$.^{1,9,10} For **Pt-3**, near-IR emission at 780 nm was observed

(Table 1). Thus we propose that the emissive triplet excited states of **Pt-3** and **Pt-4** are drastically different from those of other complexes. Based on the steady state spectroscopy and DFT calculations, we proposed a ^3IL emissive excited state for **Pt-3** and **Pt-4**. This assignment was supported by the exceptionally prolonged T_1 state lifetime of **Pt-3** and **Pt-4**, 66.7 μs and 54.7 μs , respectively, compared to the other complexes (Table 1). Such an exceptionally long-lived T_1 state is usually the feature of the ^3IL excited state.^{12,25,30–33} Furthermore, the fluorescence of the ligand was completely quenched, which is an indication of the efficient intersystem crossing (ISC). It should be pointed out that with large ligands, such as for the complexes studied in this manuscript, it is very likely that the fluorescence of the ligands cannot be quenched completely.³⁴

To the best of our knowledge, this is the first time that the anthracene-related RT phosphorescence was observed.

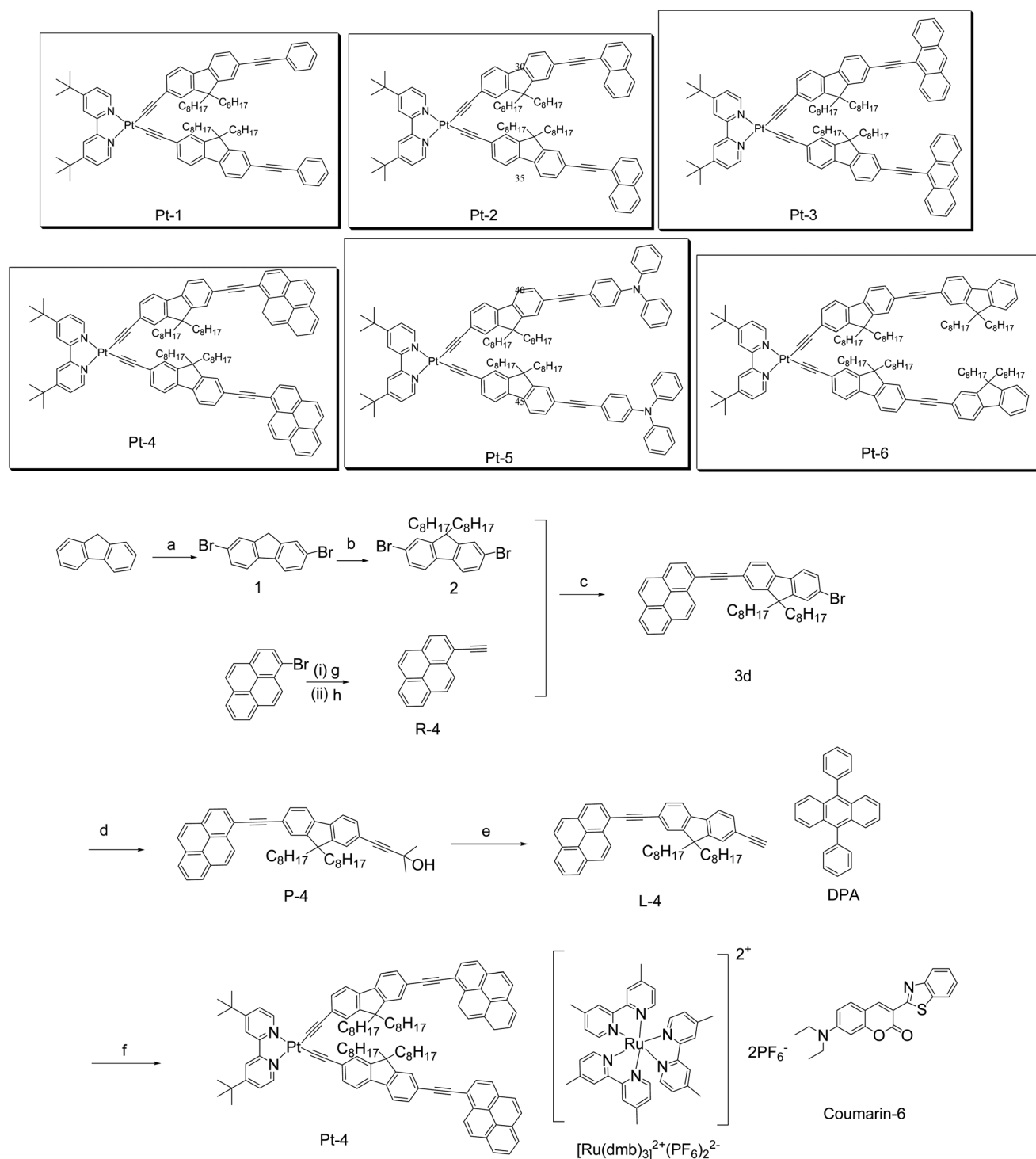
Previously anthracene was incorporated into Ru(II) bispyrene complexes, but very often the phosphorescence of the Ru(II) complexes was quenched and no emissions due to the anthracene were observed.²⁸ We attribute the RT emission of the anthracene-related ^3IL excited state to the enhanced heavy atom effect on anthracene in **Pt-3**, in which the π -conjugation core of anthracene is directly connected to the Pt(II) center. Previously the anthracene moiety was dangled on the periphery of Ru(II) complexes,^{28,35} thus we anticipated that the heavy atom effect of Ru(II) on anthracene in those complexes is weak, as a result no emission from the anthracene moiety can be observed even though the anthracene-localized ^3IL state was populated upon photoexcitation, *via* the $^1\text{MLCT} \rightarrow ^3\text{MLCT} \rightarrow ^3\text{IL}$ ISC and internal conversion (IC). This observation of the organic chromophore-localized ^3IL emission is in line with our recent observation of similar ligand localized emission in Pt(II) complexes.^{12,14,15}

Interestingly, we found the energy levels of the T_1 excited state of these fluorene-containing complexes do not decrease compared to the analogue complexes without the fluorene moieties, despite the red-shifted UV-vis absorption of the new complexes. For example, the emission band of **Pt-4** is at 663 nm. By comparison, the analogue dbbpy Pt(II) bispyrenylacetylide gives emission at 655 nm.²⁵ Furthermore, **Pt-1** emits at 592 nm, by comparison dbbpy Pt(II) bisphenylacetylide emits at 570 nm.¹⁰ This is interesting because the energy levels of the T_1 excited states of the $N^{\wedge}N$ Pt(II) bisacetylide complexes usually decrease sharply with red-shift of the UV-vis absorption.¹⁵ Keeping the T_1 at a high energy level is important for applications because a higher excited state energy level is crucial for many photo-physical processes, such as triplet energy transfer, photovoltaics, sensitizers, *etc.*

The emission of the complexes can be significantly quenched by O_2 , this is a clear indication of the phosphorescence feature of the emissions (Fig. 3).^{13,14,30,31,36,37} The emission of **Pt-4** is more sensitive to oxygen than the other complexes, indicating longer emission lifetime for **Pt-4**.^{13,30,31,33} This is in agreement with the photophysical data of the complexes (Table 1).

Emission spectra at 77 K

In order to clarify the feature of the emissive triplet excited state of the complexes, the emissions at 77 K were also



Scheme 1 Synthesis of the Pt(II) complexes **Pt-1**, **Pt-2**, **Pt-3**, **Pt-4**, **Pt-5** and **Pt-6**. (a) Br₂, CHCl₃, r.t., 12 h. (b) Octyl bromide, TBAB, aqueous NaOH (w/w = 50%), toluene, reflux; (c) Pd(PPh₃)₂Cl₂, CuI, PPh₃, NEt₃, reflux, 8 h; (d) 3-methyl-1-butyn-3-ol, Pd(PPh₃)₂Cl₂, PPh₃, CuI, NEt₃, reflux, 12 h; (e) 2-propanol, KOH, reflux, 4 h; (f) CH₂Cl₂, CuI, (i-Pr)₂NH, r.t., 12 h; (g) Pd(PPh₃)₄, CuI, trimethylsilylacetylene, NEt₃, reflux, 8 h; (h) K₂CO₃, CH₃OH, CH₂Cl₂, 3 h. The triplet acceptor 9,10-diphenylanthracene (DPA) and the quantum yield standard coumarin-6 used in the TTA upconversion are also shown.

studied and were compared with those at RT (Fig. 4).²⁵ For all the complexes the emissions at 77 K become more structured than those at RT. For **Pt-1**, the emission band gives a blue shift of 43 nm at 77 K, the large thermally induced Stokes shift (ΔE_s) of 132 cm⁻¹ indicates that the ³MLCT

component of **Pt-1** is significant. For **Pt-2** and **Pt-4**, however, the ΔE_s values are very small (9 cm⁻¹ and 5 cm⁻¹, respectively). Thus we propose that the emissions of **Pt-2** and **Pt-4** are due to the emissive triplet excited state with significant ³IL feature.²⁵

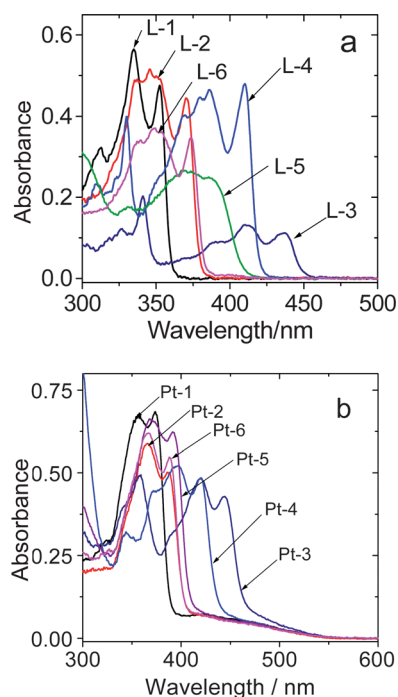


Fig. 1 UV-vis absorption spectra of (a) the ligands **L-1**, **L-2**, **L-3**, **L-4**, **L-5** and **L-6**, $c = 1.0 \times 10^{-5}$ M and (b) the complexes **Pt-1**, **Pt-2**, **Pt-3**, **Pt-4**, **Pt-5** and **Pt-6**, $c = 5.0 \times 10^{-6}$ M. In toluene, 25 °C.

Nanosecond time-resolved difference absorption spectra

The nanosecond time-resolved transient difference absorption spectra of the complexes were studied (Fig. 5). Bleaching of the ground state absorption was observed for the complexes. The transient profile of the anthracene-containing **Pt-3** is similar to that of the anthracene-containing Ru(II) complexes, thus the T_1 state of **Pt-3** can be assigned as the anthracene–fluorene localized ^3IL excited state. Furthermore, the transient absorption of **Pt-4** is similar to a N^*N Pt(II) bis(pyrenylacetylide) complex, which was proven to show the pyrene localized ^3IL triplet excited state, thus the T_1 state of the **Pt-4** can be assigned as the pyrene–fluorene localized ^3IL excited state.²⁵

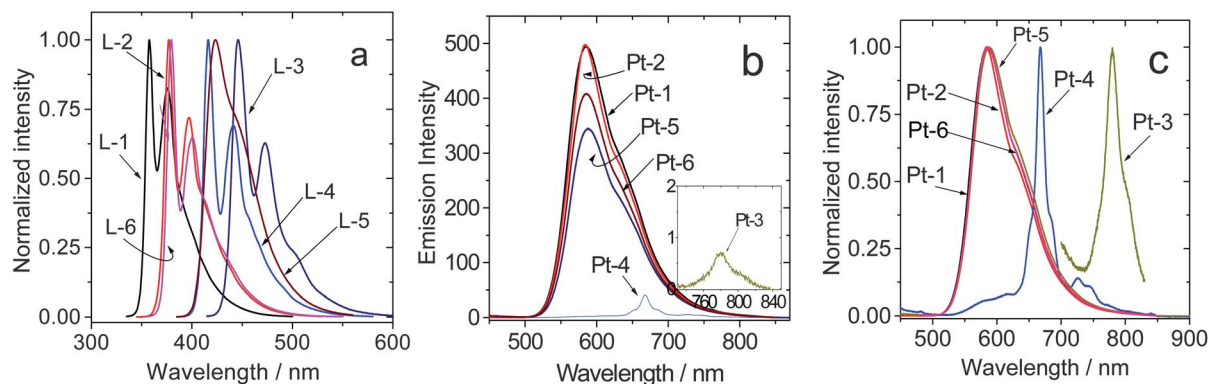


Fig. 2 (a) The normalized emission spectra of ligands **L-1**, $\lambda_{\text{ex}} = 335$ nm, **L-2**, $\lambda_{\text{ex}} = 345$ nm, **L-3**, $\lambda_{\text{ex}} = 410$ nm, **L-4**, $\lambda_{\text{ex}} = 385$ nm, **L-5**, $\lambda_{\text{ex}} = 370$ nm and **L-6**, $\lambda_{\text{ex}} = 355$ nm, $c[\text{ligands}] = 1.0 \times 10^{-5}$ M in toluene, 25 °C. (b) The phosphorescence emission and (c) the normalized emission spectra of complexes **Pt-1**, $\lambda_{\text{ex}} = 380$ nm, **Pt-2**, $\lambda_{\text{ex}} = 390$ nm, **Pt-3**, $\lambda_{\text{ex}} = 445$ nm, **Pt-4**, $\lambda_{\text{ex}} = 420$ nm, **Pt-5**, $\lambda_{\text{ex}} = 390$ nm and **Pt-6**, $\lambda_{\text{ex}} = 390$ nm. $c[\text{complexes}] = 1.0 \times 10^{-5}$ M in toluene, 25 °C.

Spin density surface of the complexes

In order to study the T_1 state of the complexes from a theoretical perspective, the spin densities of the triplet states of the complexes were studied (Fig. 6).³⁸ For complexes **Pt-1**, **Pt-2**, **Pt-5** and **Pt-6**, the spin density isosurfaces are distributed on the dbbpy ligand, Pt(II) center and the acetylide ligands, thus the triplet state of these complexes can be assigned as the typical $^3\text{MLCT}$ for the N^*N Pt(II) bisacetylide complexes. For the complexes **Pt-3** and **Pt-4**, however, the spin density isosurfaces are localized on the anthracene–fluorene or the pyrene–fluorene ligands, the dbbpy ligand and the Pt(II) center do not contribute to the spin density isosurfaces, thus the triplet state of these complexes can be assigned as the ligand-localized ^3IL state.³⁸ This conclusion is in line with the steady state and the time-resolved spectra of the complexes.

Application for triplet–triplet annihilation upconversion

Since we have shown that the fluorene-containing Pt(II) bisacetylide complexes show enhanced absorption in the visible region and long-lived triplet excited states, especially for **Pt-3** and **Pt-4**, these complexes are used as triplet sensitizers for TTA based upconversion.^{39–49} TTA upconversion is in particular interesting among the upconversion approaches, such as the two-photon absorption dyes (TPA) or the rare earth materials, for which either a very high excitation power density has to be used (10^6 W cm^{-2}),⁵⁰ or very often a low upconversion quantum yield was observed. Furthermore, it is difficult to tune the excitation/emission wavelength of these upconversion schemes. For the TTA upconversion, however, low excitation power is sufficient, the excitation power density can be down to mW cm^{-2} , on the same order of the terrestrial solar light.⁵¹ Furthermore, the excitation/emission wavelength of the TTA upconversion scheme can be readily tuned, simply by independent selection of the triplet sensitizers and triplet acceptors (but the energy levels of the sensitizer and the acceptor must be matched).⁴²

However, we noticed that the development of the TTA upconversion is facing some challenges, for example, the triplet sensitizers are very limited, currently the typical sensitizers are limited to the Pt(II)/Pd(II) porphyrin complexes.⁵² Unfortunately,

Table 1 Photophysical parameters of the ligands and the platinum complexes

$\lambda_{\text{abs}}^a/\text{nm}$	$\epsilon/10^4 \text{ M}^{-1} \text{ cm}^{-1}$	$\lambda_{\text{em}}/\text{nm}$		Φ	τ_{L}^f	
		298 K	77 K			
L-1	334/351	5.59/4.56	357/367 ^a	— ^c	0.843 ^d	3.86 ns
L-2	350/370	5.00/4.44	377/397 ^a	— ^c	0.764 ^d	0.95 ns
L-3	341/410/436	2.05/1.32/1.11	445/472 ^a	— ^c	0.687 ^d	2.44 ns
L-4	329/385/410	3.81/4.58/4.80	416/441 ^a	— ^c	0.612 ^d	1.18 ns
L-5	371/386	2.61/2.49	413 ^a	— ^c	0.858 ^d	1.02 ns
L-6	348/373	3.67/3.45	379/400 ^a	— ^c	0.723 ^d	0.73 ns
Pt-1	358/374/432	13.36/13.70/1.38	592 ^b	546/587/598 ^b	0.179 ^e	0.51 μs
Pt-2	366/389/431	11.80/9.92/1.26	574/610 ^b	571/613/627/65 ^b	0.118 ^e	1.73 μs
Pt-3	358/420/445	9.84/9.64/8.54	780 ^b	777/800 ^b	0.000 ^e	66.7 μs ^g
Pt-4	344/396/420	6.46/10.40/9.70	665/680/723/744 ^b	663/682/700/722/744 ^b	0.000 ^e	54.7 μs ^g
Pt-5	371/393/460	13.10/12.44/1.02	562 ^b	562/610 ^b	0.113 ^e	0.56 μs
Pt-6	366/389/470	12.36/10.86/0.86	564 ^b	569/645 ^b	0.156 ^e	0.72 μs

^a Recorded in toluene at 298 K. ^b Recorded in deaerated EtOH : MeOH = 4 : 1 (v/v). ^c Not determined. ^d Result in deaerated toluene solution, with quinine sulfate ($\Phi = 0.546$ in 0.05 M sulfuric acid) as the standard. ^e Result in deaerated toluene solution, with the complex $[\text{Ru}(\text{dmb})_3]^{2+}$ ($\Phi = 0.073$ in MeCN) as the standard (the solution is purged with Ar for about 15 min before measurement). ^f Luminescence lifetimes. ^g Too weak to be determined accurately with the luminescence method. Determined with the nanosecond time-resolved transient difference absorption spectroscopy.

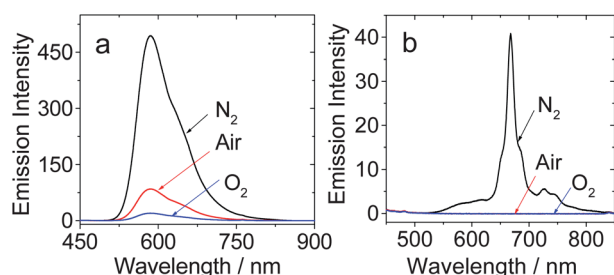


Fig. 3 Emission spectra of (a) **Pt-1**, $\lambda_{\text{ex}} = 380 \text{ nm}$, (b) **Pt-4**, $\lambda_{\text{ex}} = 420 \text{ nm}$, $c = 1.0 \times 10^{-5} \text{ M}$ under different atmospheres of nitrogen, air and oxygen (the solution is purged with Ar or O₂ for about 15 min before measurement) in toluene, 25 °C.

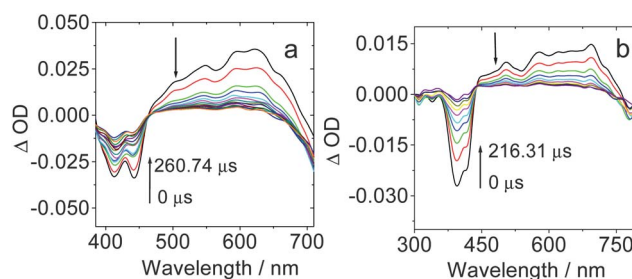


Fig. 5 Nanosecond time-resolved transient absorption difference spectra of (a) **Pt-3** and (b) **Pt-4** excited with 355 nm pulsed-laser. $c = 1.0 \times 10^{-5} \text{ M}$ in toluene, 25 °C.

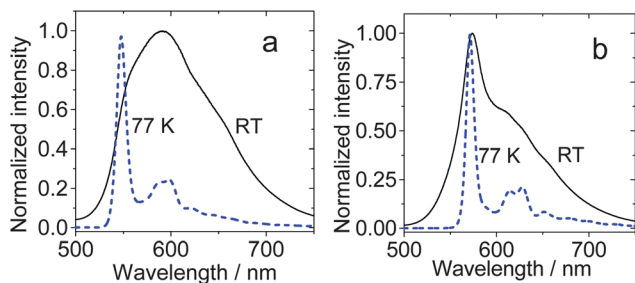


Fig. 4 Emission spectra of the complexes at 77 K and room temperature (25 °C). (a) **Pt-1**, $\lambda_{\text{ex}} = 380 \text{ nm}$, (b) **Pt-2**, $\lambda_{\text{ex}} = 390 \text{ nm}$. $c[\text{complexes}] = 1.0 \times 10^{-5} \text{ M}$ in EtOH : MeOH = 4 : 1 (v/v).

it is difficult to tune the T₁ state energy level for these complexes by modification of the molecular structures. Furthermore, the absorptions of these complexes in the visible region are usually weak. Thus, it is highly desired to develop new triplet sensitizers with readily tunable T₁ state energy levels, as well as intense absorption in the visible region.

Firstly the emissions of the complexes upon 445 nm laser excitation were studied (Fig. 7). **Pt-1**, **Pt-2**, **Pt-5** and **Pt-6** give strong emission at ca. 600 nm. Notably **Pt-4** is weakly luminescent and **Pt-3** is nonluminescent (Fig. 7a). In the presence of the

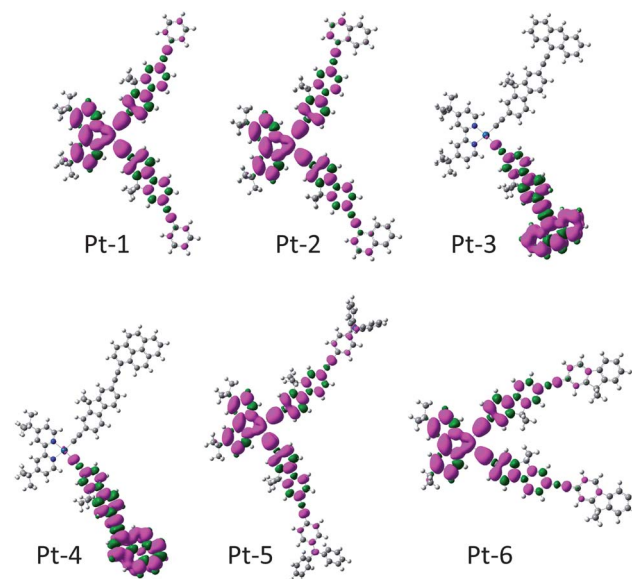


Fig. 6 The spin density of **Pt-1**, **Pt-2**, **Pt-3**, **Pt-4**, **Pt-5** and **Pt-6** based on the optimized triplet state geometry. Calculation is based on DFT at the B3LYP/6-31G(d)/LanL2DZ level using Gaussian 09W.

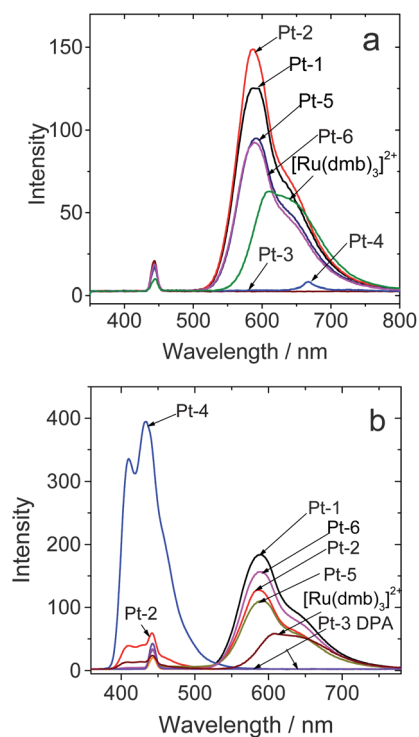


Fig. 7 Emission and upconversion with the complexes as triplet sensitizers upon 445 nm laser excitation. (a) Emission of the Pt(II) complexes without DPA. (b) Upconverted emission in the presence of DPA, $\lambda_{\text{ex}} = 445$ nm, 5 mW, $c[\text{sensitizer}] = 1.0 \times 10^{-5}$ M, $c[\text{DPA}] = 4.3 \times 10^{-5}$ M in toluene, 25 °C.

triplet acceptor DPA, intense blue emissions in the range of 400–550 nm were found (Fig. 7a). Irradiation of DPA alone with a 445 nm laser does not produce blue emission. Thus the blue emission with **Pt-4** can be assigned as the upconverted fluorescence emission with **Pt-4** as the triplet sensitizer. Minor upconversion was observed with **Pt-2** as the triplet sensitizer. For other complexes, however, the upconversion is negligible. Although the emissions of these complexes are much stronger than that of **Pt-4**, we attribute the lack of upconversion with **Pt-1** to the short T_1 state lifetime and the weak absorption at the excitation wavelength,⁴⁹ thus the population of the triplet excited sensitizers is under the threshold for TTA upconversion.

The role of the dark excited states in TTA upconversion

Interestingly, the upconverted fluorescence peak area with **Pt-4** is much higher than the quenched phosphorescent peak areas. This is abnormal because the conversionally phosphorescent triplet sensitizers are used and usually the upconverted fluorescence emission band is accompanied by the quenching of the phosphorescence.^{42,53} According to the photophysics of the TTA upconversion, the quenched phosphorescence emission band area should be at least two fold of that of the upconverted fluorescence emission band.^{42,53}

For **Pt-4**, we propose that the triplet sensitizers at the triplet excited state that are otherwise non-emissive were involved in the key photophysical process of the TTET.^{15,32,54} Actually it is unnecessary for the triplet sensitizer to be phosphorescent to sensitize the TTET process, and the phosphorescence, *i.e.* the

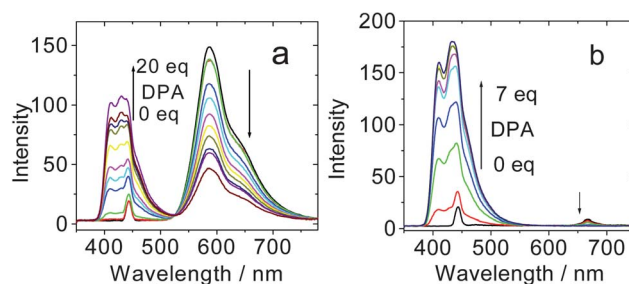


Fig. 8 The upconversion of (a) **Pt-2** and (b) **Pt-4**, $c = 1.0 \times 10^{-5}$ M with increasing DPA concentration. With 445 nm (5 mW) laser excitation. In toluene, 25 °C.

radiative decay of the T_1 state, is actually competitive to the TTET process. Thus the phosphorescence is detrimental to the TTA upconversion. Therefore, we propose that weakly phosphorescent, or non-phosphorescent transition metal complexes can be used as the triplet sensitizers for the TTA upconversion, as long as the triplet excited state of the complexes can be efficiently populated upon photoexcitation.^{15,32,54}

The dark excited state of **Pt-4** that is involved in the TTET, thus the TTA upconversion, is clearly demonstrated in Fig. 8. For **Pt-2**, with an increase in the concentration of DPA, the upconverted fluorescence emission of DPA increased with the significant quenching of the phosphorescence in the range of 550–750 nm. This quenching of the phosphorescence by DPA is reasonable since the TTET process is enhanced with more concentrated DPA and the T_1 excited state, which is responsible for the phosphorescence of **Pt-4**, is quenched. For the triplet sensitizer **Pt-4**, however, the upconverted fluorescence emission is greatly enhanced without any phosphorescence to be

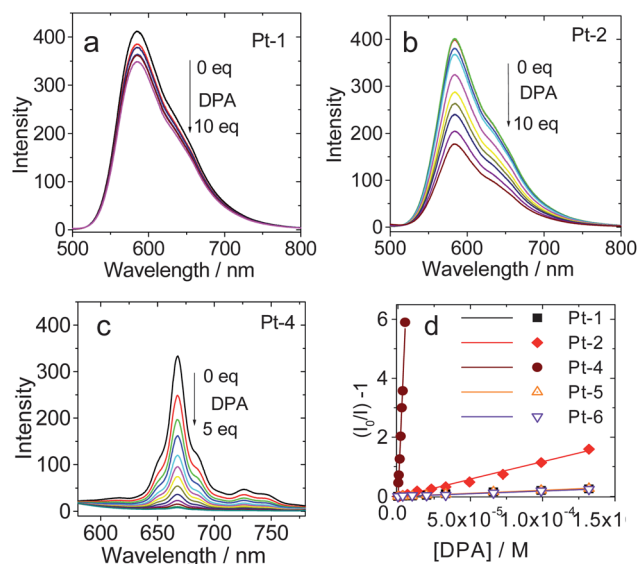


Fig. 9 Phosphorescence emission spectra of complex (a) **Pt-1**, $\lambda_{\text{ex}} = 380$ nm, (b) **Pt-2**, $\lambda_{\text{ex}} = 390$ nm, and (c) **Pt-4**, $\lambda_{\text{ex}} = 420$ nm with increasing DPA concentration in toluene. (d) Stern–Volmer plots for phosphorescence quenching of **Pt-1**, $\lambda_{\text{ex}} = 380$ nm, **Pt-2**, $\lambda_{\text{ex}} = 390$ nm, **Pt-4**, $\lambda_{\text{ex}} = 420$ nm, **Pt-5**, $\lambda_{\text{ex}} = 385$ nm and **Pt-6**, $\lambda_{\text{ex}} = 385$ nm, $c = 1.0 \times 10^{-5}$ M in toluene at 25 °C.

Table 2 Upconversion related photophysical properties of Pt(II) complexes^a

	$\tau_T/\mu\text{s}^b$	$K_{sv}/10^3 \text{ M}^{-1c}$	Φ_{UC}^d
Pt-1	0.74	1.98	0.0
Pt-2	2.02	11.89	$3.0 \pm 1.0\%$
Pt-3	66.7	—	0.0
Pt-4	54.7	1209	$22.4 \pm 3\%$
Pt-5	0.59	2.07	0.0
Pt-6	0.88	1.83	0.0
[Ru(dmb)₃]²⁺	—	—	$0.5 \pm 0.3\%$

^a Recorded in deaerated toluene at 298 K. ^b Triplet state lifetime. ^c Stern–Volmer quenching constants for phosphorescence quenching. ^d Upconversion quantum yields, with coumarin 6 as the standard ($\Phi = 0.78$ in $\text{CH}_3\text{CH}_2\text{OH}$).

quenched. Thus the gain of the upconversion can only be rationalized by the involvement of the dark excited state, *i.e.* those non-radiative T_1 excited states of **Pt-4**, in the TTET process. This new concept of using non-phosphorescent triplet sensitizers for TTA upconversion will greatly broaden the availability of the triplet sensitizers for TTA upconversion, and other photophysical processes that require a triplet excited state to initiate.

The efficiency of the TTET process

The TTET process was studied by the quenching of the phosphorescence of sensitizers with DPA (Fig. 9).^{14,15,49,54} For **Pt-1**, the phosphorescence peak was quenched slightly. For **Pt-2**, the quenching by increasing the DPA concentration is significant. The most significant quenching was observed for **Pt-4**. With 5 eq. of DPA, the phosphorescence peak is almost completely quenched. The quenching effect on the phosphorescence of the triplet sensitizers can be quantified by the construction of the

quenching curves following the Stern–Volmer equation (Fig. 9d). A quenching constant of $1.19 \times 10^4 \text{ M}^{-1}$ was determined for **Pt-2**. For **Pt-4**, however, a much higher quenching constant of $1.21 \times 10^6 \text{ M}^{-1}$ was observed. Thus the significant upconversion with **Pt-4** as the triplet sensitizer can be attributed to its strong absorption and the efficient TTET process (Table 2).

Recently a $N^{\wedge}N^{\wedge}N$ Pt(II) acetylide complex was reported as a triplet sensitizer for TTA upconversion, but the upconversion quantum yield is much lower (less than 2%).⁵⁵ This low upconversion quantum yield is due to the weak absorption of the complex at the excitation wavelength, and the short T_1 excited state lifetime (4.8 μs).

The upconversion with the complexes as the triplet sensitizer is visible with unaided eyes (Fig. 10). For complexes **Pt-1**, **Pt-2**, **Pt-5** and **Pt-6**, yellow emission was observed for the sensitizer solution upon 445 nm laser excitation. For the complexes **Pt-3** and **Pt-4**, however, blue beam paths were observed, which is due to the weak emission of the two complexes and the scattered laser light. In the presence of the triplet acceptor DPA, the emission color of the beam path for **Pt-1**, **Pt-5** and **Pt-6** is yellow, due to the lack of the upconversion with these complexes. For **Pt-2**, the emission colour is close to white, due to the upconverted fluorescence emission and the residual phosphorescence emission. Intense blue emission was observed for **Pt-4**, due to its intense upconversion.

The upconversion with the Pt(II) bisacetylide complex as the triplet sensitizer can be summarized in Scheme 2. Photoexcitation of **Pt-4** produces the sensitizers at the ^1IL singlet excited state. Then with ISC, the triplet excited state ^3IL , most probably *via* $^3\text{MLCT}$, was populated. Then the TTET occurred between the ^3IL excited state of the sensitizer and the DPA triplet acceptor. The light-harvesting ability of the sensitizer will produce more concentrated sensitizer molecules at the triplet

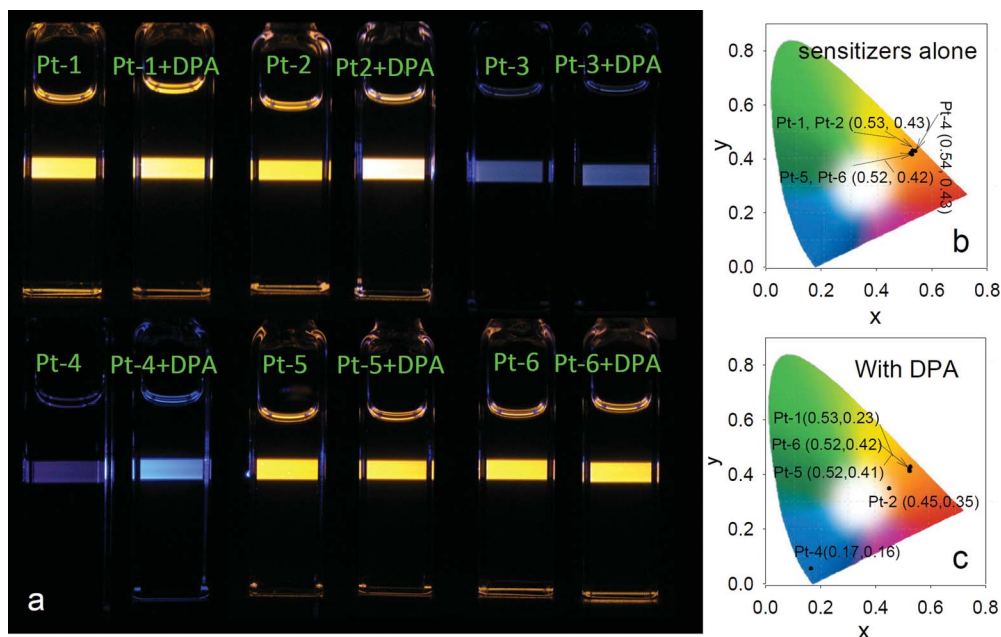
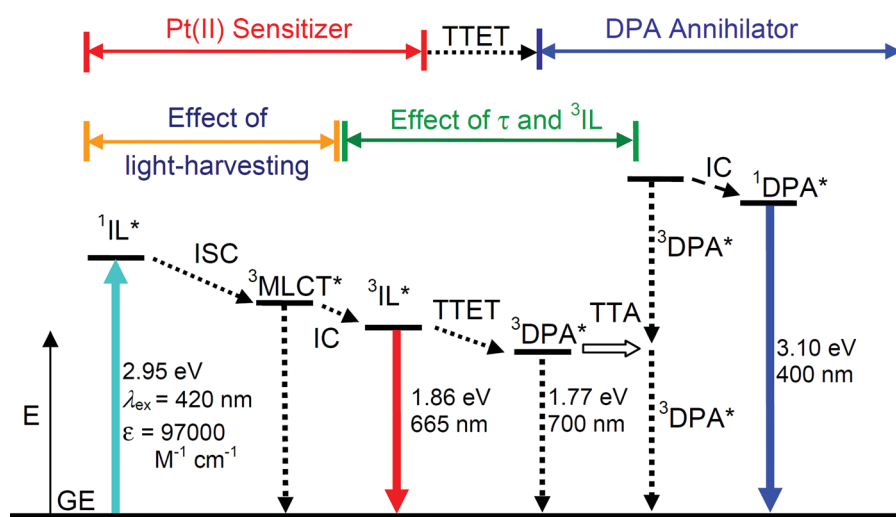


Fig. 10 Photographs of the upconversion with the Pt(II) complexes as triplet sensitizers. (a) Images before and after adding DPA of **Pt-1**, **Pt-2**, **Pt-3**, **Pt-4**, **Pt-5** and **Pt-6** in toluene. (b) The CIE of **Pt-1**, **Pt-2**, **Pt-3**, **Pt-4**, **Pt-5** and **Pt-6** emission and (c) the CIE of the upconversion. $c[\text{complexes}] = 1.0 \times 10^{-5} \text{ M}$, $c[\text{DPA}] = 4.33 \times 10^{-5} \text{ M}$, 25°C .



Scheme 2 Qualitative Jablonski diagram illustrating the sensitized TTA upconversion process between Pt(II) complexes (exemplified by **Pt-4**) and DPA. The effect of the light-harvesting ability and the luminescence lifetime of the Pt(II) sensitizer on the efficiency of the TTA upconversion is also shown. Please note that **Pt-4** shows absorption at 420 nm, but it is excitable at 445 nm (laser was used for upconversion). *E* is energy. GS is ground state (S_0). $^1\text{IL}^*$ is intraligand singlet excited state (fluorene-pyrenyl localized). IC is intersystem conversion. $^3\text{MLCT}^*$ is the Pt(II) based metal-to-ligand-charge-transfer triplet excited state. $^3\text{IL}^*$ is intraligand triplet excited state (fluorene-pyrenyl localized). TTET is triplet-triplet energy transfer. $^3\text{DPA}^*$ is the triplet excited state of DPA. TTA is triplet-triplet annihilation. $^1\text{DPA}^*$ is the singlet excited state of DPA. The emission bands observed for the sensitizers alone are the ^3IL emissive excited state. The emission bands observed in the TTA experiment are the simultaneous $^3\text{IL}^*$ emission (phosphorescence) and the $^1\text{DPA}^*$ emission (fluorescence).

excited state, whereas the long-lifetime of the T_1 excited state of the sensitizer can enhance the TTET process. Thus the light-harvesting ability of the complexes and the lifetime are important for the TTA upconversion. The collision of the DPA molecules will produce the singlet excited state, in a probability of 11.1%, determined by the spin statistic rule.^{43,54} Radiative decay of the singlet excited state of the DPA molecules will produce the fluorescence emission, for which the wavelength is shorter than the excitation wavelength.

Conclusions

Fluorene-containing aryl acetylides were used to prepare $N^{\wedge}N$ Pt(II) bisacetylides complexes, where aryl substituents on the fluorene moiety are phenyl, naphthal, anthranyl, pyrenyl, 4-diphenylaminophenyl and 9,9-di-*n*-octylfluorene (where $N^{\wedge}N$ ligand = 4,4'-di-*tert*-butyl-2,2'-bipyridine). All the complexes show room temperature (RT) phosphorescence. The emissive T_1 excited state of the complexes **Pt-1**, **Pt-5** and **Pt-6** was assigned as the $^3\text{MLCT}$ state, whereas for **Pt-2**, **Pt-3** and **Pt-4**, the emissive T_1 excited states were identified with the ^3IL as the major components, based on the steady state emission spectra, the lifetime of the T_1 state, the emission spectra at 77 K, the spin density analysis and the time-resolved transient absorption spectroscopy. Exceptionally long-lived T_1 excited states were observed for complexes containing anthranyl ($\tau = 66.7 \mu\text{s}$) or pyrenyl acetylides ($\tau = 54.7 \mu\text{s}$), compared to the other complexes (less than 2.0 μs). RT phosphorescence of anthracene was observed at 780 nm with complex **Pt-3**. We found that with fluorene substitution, the absorption of the complexes is red-shifted compared to the analogues, without compromising the T_1 energy levels. The advantage of this unique spectral tuning effect and the long-lived T_1 excited states of **Pt-4** were demonstrated by

the enhanced performance as triplet sensitizer for triplet-triplet-annihilation based upconversion; an upconversion quantum yield of 22.4% was observed, in stark contrast to the previously reported upconversion quantum yields for the transition metal complexes of less than 20%. Other complexes described herein show negligible upconversion. The high upconversion quantum yield of **Pt-4** is attributed to its intense absorption of visible light, long-lived T_1 excited state and appropriate T_1 state energy level. Based on the result of **Pt-4**, we propose that weakly phosphorescent, or non-phosphorescent transition metal complexes can be used as triplet sensitizers for TTA upconversion, vs. the typical phosphorescent triplet sensitizers. Our results will be useful for the rational design of transition metal complexes to enhance the light-absorption, without decreasing the T_1 excited state energy levels, which is important for the application of the complexes as triplet sensitizers in various photophysical processes.

Acknowledgements

We thank the NSFC (20972024, 21073028 and 21103015), the Fundamental Research Funds for the Central Universities (DUT10ZD212 and DUT11LK19), Ministry of Education (SRFDP-200801410004 and NCET-08-0077), the Royal Society (UK) and NSFC (China-UK Cost-Share Science Networks, 21011130154), the Education Department of Liaoning Province (2009T015) and Dalian University of Technology for financial support.

References

- 1 J. A. G. Williams, *Top. Curr. Chem.*, 2007, **281**, 205.
- 2 J. Zhang, P. Du, J. Schneider, P. Jarosz and R. Eisenberg, *J. Am. Chem. Soc.*, 2007, **129**, 7726.

- 3 J. E. McGarrah, Y.-J. Kim, M. Hissler and R. Eisenberg, *Inorg. Chem.*, 2001, **40**, 4510.
- 4 W.-Y. Wong and C.-L. Ho, *Acc. Chem. Res.*, 2010, **43**, 1246.
- 5 Q. Zhao, F. Li and C. Huang, *Chem. Soc. Rev.*, 2010, **39**, 3007.
- 6 Y. Chen, K. Li, W. Lu, S. S.-Y. Chui, C.-W. Ma and C. Che, *Angew. Chem., Int. Ed.*, 2009, **48**, 9909.
- 7 R. Zhang, Z. Ye, G. Wang, W. Zhang and J. Yuan, *Chem.–Eur. J.*, 2010, **16**, 6884.
- 8 S. Ji, H. Guo, X. Yuan, X. Li, H. Ding, P. Gao, C. Zhao, W. Wu, W. Wu and J. Zhao, *Org. Lett.*, 2010, **12**, 2876.
- 9 C. E. Whittle, J. A. Weinstein, M. W. George and K. S. Schanze, *Inorg. Chem.*, 2001, **40**, 4053.
- 10 M. Hissler, W. B. Connick, D. K. Geiger, J. E. McGarrah, D. Lipa, R. J. Lachicotte and R. Eisenberg, *Inorg. Chem.*, 2000, **39**, 447.
- 11 F. N. Castellano, I. E. Pomestchenko, E. Shikhova, F. Hua, M. L. Muro and N. Rajapakse, *Coord. Chem. Rev.*, 2006, **250**, 1819.
- 12 H. Guo, M. L. Muro-Small, S. Ji, J. Zhao and F. N. Castellano, *Inorg. Chem.*, 2010, **49**, 6802.
- 13 H. Guo, S. Ji, W. Wu, W. Wu, J. Shao and J. Zhao, *Analyst*, 2010, **135**, 2832.
- 14 H. Sun, H. Guo, W. Wu, X. Liu and J. Zhao, *Dalton Trans.*, 2011, **40**, 7834.
- 15 Y. Liu, W. Wu, J. Zhao, X. Zhang and H. Guo, *Dalton Trans.*, 2011, **40**, 9085.
- 16 G. Zhou, W.-Y. Wong, S.-Y. Poon, C. Ye and Z. Lin, *Adv. Funct. Mater.*, 2009, **19**, 531.
- 17 J. B. Seneclauze, P. Retailleau and R. Ziessel, *New J. Chem.*, 2007, **31**, 1412.
- 18 Z. Ji, S. Li, Y. Li and W. Sun, *Inorg. Chem.*, 2010, **49**, 1337.
- 19 Z. Zhao, X. Xu, Z. Jiang, P. Lu, G. Yu and Y. Liu, *J. Org. Chem.*, 2007, **72**, 8345.
- 20 S. Tao, Y. Zhou, C.-S. Lee, X. Zhang and S.-T. Lee, *Chem. Mater.*, 2010, **22**, 2138.
- 21 J. E. Haley, D. M. Krein, J. L. Monahan, A. R. Burke, D. G. McLean, J. E. Slagle, A. Fratini and T. M. Cooper, *J. Phys. Chem. A*, 2011, **115**, 265.
- 22 G.-J. Zhou and W.-Y. Wong, *Chem. Soc. Rev.*, 2011, **40**, 2541.
- 23 Y. Qu, J. Hua and H. Tian, *Org. Lett.*, 2010, **12**, 3320.
- 24 M. G. Frisch, G. W. Trucks and H. B. Schlegel, *et al.*, *Gaussian 09W Revision A.1*, Gaussian Inc, Wallingford, CT, 2009.
- 25 I. E. Pomestchenko, C. R. Luman, M. Hissler, R. Ziessel and F. N. Castellano, *Inorg. Chem.*, 2003, **42**, 1394.
- 26 N. Armaroli, *ChemPhysChem*, 2008, **9**, 371.
- 27 D. V. Kozlov, D. S. Tyson, C. Goze, R. Ziessel and F. N. Castellano, *Inorg. Chem.*, 2004, **43**, 6083.
- 28 G. J. Wilson, A. Launikonis, W. H. F. Sasse and A. W.-H. Mau, *J. Phys. Chem. A*, 1997, **101**, 4860.
- 29 X. Han, L.-Z. Wu, G. Si, J. Pan, Q.-Z. Yang, L.-P. Zhang and C.-H. Tung, *Chem.–Eur. J.*, 2007, **13**, 1231.
- 30 S. Ji, W. Wu, W. Wu, P. Song, K. Han, Z. Wang, S. Liu, H. Guo and J. Zhao, *J. Mater. Chem.*, 2010, **20**, 1953.
- 31 W. Wu, W. Wu, S. Ji, H. Guo, P. Song, K. Han, L. Chi, J. Shao and J. Zhao, *J. Mater. Chem.*, 2010, **20**, 9775.
- 32 J. Sun, W. Wu, H. Guo and J. Zhao, *Eur. J. Inorg. Chem.*, 2011, 3165.
- 33 W. Wu, W. Wu, S. Ji, H. Guo and J. Zhao, *Dalton Trans.*, 2011, **40**, 5953.
- 34 D. N. Kozhevnikov, V. N. Kozhevnikov, M. Z. Shafikov, A. M. Prokhorov, D. W. Bruce and J. A. G. Williams, *Inorg. Chem.*, 2011, **50**, 3804.
- 35 A. F. Morales, G. Accorsi, N. Armaroli, F. Barigelletti, S. J. A. Pope and M. D. Ward, *Inorg. Chem.*, 2002, **41**, 6711.
- 36 W. Wu, W. Wu, S. Ji, H. Guo and J. Zhao, *J. Organomet. Chem.*, 2011, **696**, 2388.
- 37 W. Wu, S. Ji, W. Wu, H. Guo, X. Wang, J. Zhao and Z. Wang, *Sens. Actuators, B*, 2010, **149**, 395.
- 38 K. Hanson, A. Tamayo, V. V. Diev, M. T. Whited, P. I. Djurovich and M. E. Thompson, *Inorg. Chem.*, 2010, **49**, 6077.
- 39 L. Huang, L. Zeng, H. Guo, W. Wu, W. Wu, S. Ji and J. Zhao, *Eur. J. Inorg. Chem.*, 2011, 4527.
- 40 W. Wu, J. Sun, S. Ji, W. Wu, J. Zhao and H. Guo, *Dalton Trans.*, 2011, **40**, 11550.
- 41 J. Zhao, S. Ji and H. Guo, *RSC Adv.*, 2011, **1**, 937.
- 42 T. N. Singh-Rachford and F. N. Castellano, *Coord. Chem. Rev.*, 2010, **254**, 2560.
- 43 A. Monguzzi, J. Mezyk, F. Scotognella, R. Tubino and F. Meinardi, *Phys. Rev. B: Condens. Matter Mater. Phys.*, 2008, **78**, 195112.
- 44 Y. Y. Cheng, T. Khoury, R. G. C. R. Clady, M. J. Y. Tayebjee, N. J. Ekins-Daukes, M. J. Crossley and T. W. Schmidt, *Phys. Chem. Chem. Phys.*, 2010, **12**, 66.
- 45 R. R. Islangulov, D. V. Kozlov and F. N. Castellano, *Chem. Commun.*, 2005, 3776.
- 46 H.-C. Chen, C.-Y. Hung, K.-H. Wang, H.-L. Chen, W. S. Fann, F.-C. Chien, P. Chen, T. J. Chow, C.-P. Hsu and S.-S. Sun, *Chem. Commun.*, 2009, 4064.
- 47 T. N. Singh-Rachford, R. R. Islangulov and F. N. Castellano, *J. Phys. Chem. A*, 2008, **112**, 3906.
- 48 K. Tanaka, K. Inafuku and Y. Chujo, *Chem. Commun.*, 2010, **46**, 4378.
- 49 S. Ji, W. Wu, W. Wu, H. Guo and J. Zhao, *Angew. Chem., Int. Ed.*, 2011, **50**, 1626.
- 50 H. M. Kim and B. R. Cho, *Acc. Chem. Res.*, 2009, **42**, 863.
- 51 S. Balushev, V. Yakutkin, T. Miteva, Y. Avlasevich, S. Chernov, S. Aleshchenkov, G. Nelles, A. Cheprakov, A. Yasuda, K. Müllen and G. Wegner, *Angew. Chem., Int. Ed.*, 2007, **46**, 7693.
- 52 T. N. Singh-Rachford, A. Haefele, R. Ziessel and F. N. Castellano, *J. Am. Chem. Soc.*, 2008, **130**, 16164.
- 53 Y. Y. Cheng, B. Fckel, T. Khoury, R. G. C. R. Clady, M. J. Y. Tayebjee, N. J. Ekins-Daukes, M. J. Crossley and T. W. Schmidt, *J. Phys. Chem. Lett.*, 2010, **1**, 1795.
- 54 S. Ji, H. Guo, W. Wu, W. Wu and J. Zhao, *Angew. Chem., Int. Ed.*, 2011, **50**, 8283.
- 55 P. Du and R. Eisenberg, *Chem. Sci.*, 2010, **1**, 502.